Human Molecular Genetics, 2003, Vol. 12, No. 16 **1945–1958**
DOI: 10.1093/hmg/ddg211

Ubiquitin carboxy-terminal hydrolase L1 binds to and stabilizes monoubiquitin in neuron

Hitoshi Osaka[1,2,†,‡], Yu-Lai Wang[1,†], Koji Takada[3], Shuichi Takizawa[1,4], Rieko Setsuie[1,5], Hang Li[1], Yae Sato[1,5], Kaori Nishikawa[1], Ying-Jie Sun[1], Mikako Sakurai[1,5], Takayuki Harada[1], Yoko Hara[1,6], Ichiro Kimura[6], Shigeru Chiba[4], Kazuhiko Namikawa[7], Hiroshi Kiyama[7], Mami Noda[5], Shunsuke Aoki[1] and Keiji Wada[1,*]

[1]Department of Degenerative Neurological Diseases, National Institute of Neuroscience, National Center of Neurology and Psychiatry, Kodaira, Tokyo, 187-8502, Japan, [2]Information and Cellular function, PRESTO, Japan Science and Technology Corporation (JST), Kawaguchi, Saitama 332-0012, Japan, [3]Department of Biochemistry 1, Jikei University School of Medicine, Minato-ku, Tokyo, 105-8461, Japan, [4]Department of Psychiatry and Neurology, Asahikawa Medical College, Asahikawa, 078-8510, Japan, [5]Laboratory of Pathophysiology, Graduate School of Pharmaceutical Sciences, Kyushu University, Higashi-ku, Fukuoka, 812-8582, Japan, [6]Department of Basic Human Science, School of Human Science, Waseda University, Tokorozawa, 359-1192, Japan and [7]Department of Anatomy and Neurobiology, Graduate School of Medicine, Osaka City University, Abeno-ku, Osaka, 545-8585, Japan

Received March 13, 2003; Revised June 6, 2003; Accepted June 17, 2003

Mammalian neuronal cells abundantly express a deubiquitylating enzyme, ubiquitin carboxy-terminal hydrolase 1 (UCH L1). Mutations in UCH L1 are linked to Parkinson's disease as well as gracile axonal dystrophy (*gad*) in mice. In contrast to the UCH L3 isozyme that is universally expressed in all tissues, UCH L1 is expressed exclusively in neurons and testis/ovary. We found that UCH L1 associates and colocalizes with monoubiquitin and elongates ubiquitin half-life. The *gad* mouse, in which the function of UCH L1 is lost, exhibited a reduced level of monoubiquitin in neurons. In contrast, overexpression of UCH L1 caused an increase in the level of ubiquitin in both cultured cells and mice. These data suggest that UCH L1, with avidity and affinity for ubiquitin, insures ubiquitin stability within neurons. This study is the first to show the function of UCH L1 *in vivo*.

INTRODUCTION

The small 76-amino acid protein ubiquitin (Ub) plays a critical role in many cellular processes, including the cell cycle, cell proliferation, development, apoptosis, signal transduction and membrane protein internalization (1). Moreover, Ub and/or Ub-containing protein aggregates are hallmarks of various neurodegenerative conditions (2). Fundamentally, monoubiquitylation constitutes a sorting signal for membrane proteins to the endosome–lysosomal pathway while polyubiquitylated proteins (covalently linked to Lys48 of Ub) are targeted to the 26S proteasome for degradation. At least three classes of enzymes are engaged in the ubiquitylation processes, namely the E1 (Ub-activating), E2 (Ub-conjugating) and E3 (Ub ligase) enzymes (1). Ubiquitylation also controls the sorting and localization of certain proteins in a reversible manner, much as phosphorylation modulates changes in the structure, activity and the localization of the target proteins. As such, deubiquitylating enzymes (DUBs) act analogously to phosphatases that function in phosphorylation processes (3).

DUBs are subdivided into Ub C-terminal hydrolases (UCHs) and Ub-specific proteases (UBPs). Both classes are thiol proteases that hydrolyze the isopeptide bond between the substrate and the C-terminal Gly76 of Ub. UCHs can hydrolyze bonds between Ub and small adducts or unfolded polypeptides *in vitro* (4). UCHs also can cleave Ub gene products very slowly

*To whom correspondence should be addressed at: Department of Degenerative Neurological Diseases, National Institute of Neuroscience, NCNP, Kodaira, Tokyo, 187-8502, Japan. Tel: +81 423461715; Fax: +81 423461745; Email: wada@ncnp.go.jp
†The authors wish it to be known that, in their opinion, the first two authors should be regarded as joint First Authors.
‡Present address:
Division of Neurology, Clinical Research Institute, Kanagawa Children's Medical Center, Yokohama, 232-8555, Japan.

Human Molecular Genetics, Vol. 12, No. 16 © Oxford University Press 2003; all rights reserved

Downloaded from https://academic.oup.com/hmg/article/12/16/1945/2355580 by guest on 20 August 2022

in vitro, either tandemly conjugated Ub monomers (UbB, UbC) or Ub fused to small ribosomal proteins (L40, S27a), to yield free Ub or ribosomal proteins, respectively (4,5). Yeast expresses one UCH (YUH1) and 16 UBPs (Ubp1–16). Two YUH1 homologs, UCH L1 and UCH L3, have been characterized in mammals (6,7). UCH L1 and UCH L3 are both small proteins of ~220 amino acids that share more than 40% amino acid sequence identity. However, the distribution of these isozymes is quite distinct in that UCH L3 is expressed ubiquitously while UCH L1 is selectively expressed in neuronal cells and the testis/ovary (6,7).

UCH L1 is one of the most abundant proteins in the brain (1–5% of total soluble protein) and immunohistological experiments demonstrate that it is localized exclusively to neurons (6). Although the role of UCH L1 *in vivo* remains unclear, its abundance and specificity for neurons predict a role in neuronal cell function/dysfunction. Similar to Ub, UCH L1 is a constituent of cellular aggregates that are indicative of neurodegenerative disease such as Lewy bodies in Parkinson's disease (PD) (8). Indeed, an isoleucine-to-methionine substitution at amino acid 93 of UCH L1 was reported in a family with a dominant form of PD (9). We found that a *Uch l1* gene deletion in mice causes gracile axonal dystrophy (*gad*), a recessive neurodegenerative disease (10,11). These two examples of neurological disorders in both humans and mice prompted us to investigate the function of UCH L1 in neuronal cells.

We show here that the *gad* mouse is analogous to a *Uch l1* null mutant. Using this mouse and *Uch l1* transgenic mice, we report a novel *in vivo* role for UCH L1 in Ub homeostasis that was unexpected from previous *in vitro* work (12,13). Our data show that UCH L1 associates with Ub in neuronal cells and suggest that this association is important for the maintenance of mono-Ub levels in neurons. UCH L1 effectively upregulates Ub levels at the post-translational level, and this upregulation is probably based on the inhibition of Ub degradation by UCH L1.

RESULTS

UCH L1 is undetectable in the *gad* mouse

The *gad* mouse carries a deletion of a genomic fragment including exons 7 and 8 of *Uchl1* (10). Given such a substantial deletion, the protein encoded by the *gad* allele most likely lacks the core structure of UCH L1, thus predicating its instability [wild-type mouse UCH L1 was modeled using the crystal structure of human UCH L3 (14) as a template; see Fig. 1A]. Immunoblotting using polyclonal antibody to UCH L1 failed to detect UCH L1 in either soluble (10) or insoluble brain lysates from the *gad* mouse (data not shown). Thus, the *gad* mouse is analogous to a *Uch l1* null mutant. Next, we examined whether UCH L3, another UCH in the brain, is upregulated by this mutation. The *gad* mouse showed comparable levels of UCH L3 mRNA and protein (Fig. 1B). Therefore, the phenotype in the mouse does not appear to be modified by compensatory UCH L3 up-regulation. We then employed this mutant mouse to characterize UCH L1 substrates or associated proteins *in vivo.*

UCH L1 associates with Ub

There should be physiological substrates for UCH L1 that accumulate in the *gad* mouse. To facilitate isolation of such UCH L1 substrates or associated proteins, mutant UCH $L1^{C90S}$ was purified from an *E. coli* expression system. UCH $L1^{C90S}$ lacks Ub carboxy-terminal hydrolase activity but retains the ability to associate with Ub (4) (Table 1). As such, UCH $L1^{C90S}$ represented an ideal tool for the purpose of binding to and isolating *in vivo* protein substrates or associates for UCH L1. His-UCH $L1^{C90S}$ and Ni-Sepharose resin were employed in a pull-down assay using soluble brain lysates from wild-type and *gad* mice. Eluates from the resin were subjected to SDS–PAGE and SELDI (surface-enhanced laser desorption/ionization) time-of-flight (TOF) analysis. Relative to wild-type lysates, consistently elevated levels of proteins were not detected in the *gad* mice brains including putative substrates of poly-Ub. Rather, the level of an ~8 kDa protein was consistently lower in *gad* mice lysates (Fig. 1C; left panel; band intensity of *gad* to wild-type is 0.80 ± 0.09, $n = 3$). In both lysates, this protein band was immunoreactive with an antibody to Ub (Fig. 1C; right panel). In-gel digestion of this band followed by tandem liquid chromatography/mass spectrometry produced two peptide sequences—TLSYNIQKESTLHLVLR and TITLEVEPSDTIENVK—that were 100% identical to sequences within mouse Ub. In another pull-down assay, His-Ub pulled down a band corresponding to UCH L1 (Fig. 1D). SELDI analysis showed identical mass peak patterns for the Ub band from wild-type and *gad* mice (Fig. 1E) with a principal mass peak at 8560.8 *m*/*z*, consistent with the *m*/*z* expected for free mono-Ub (8564.8). Wild-type and *gad* mouse brain lysates were then subjected to gel filtration chromatography and immunoblotted with anti-UCH L1 or anti-Ub. In the fractions from the wild-type mouse, mono-Ub eluted over the range of ~10–50 kDa, overlapping significantly with the elution of UCH L1 (Fig. 1F). In fractions from the *gad* mouse, however, mono-Ub eluted exclusively at ~10–14 kDa. These data suggest that UCH L1 associates with mono-Ub.

Loss of UCH L1 decreases the level of Ub in neuron

The expression and localization of UCH L1 and mono-Ub in the mouse nerve system were examined. The nervous system is consisted of two types of cells, nerve cells (neurons) and glia (astrocytes, oligodendrocytes/schwann cells, microglia, ependymal cells). Immunofluorescence microscopy shows UCH L1 co-expresses with a neuron marker, neurofilament (NF), but not with an oligodendrocytes marker, proteolipid protein (PLP), and an astrocytes marker, glial fibrillary acidic protein (GFAP), thus supporting the neuron-specific expression of UCH L1 (6) (Fig. 2A). Then double immunofluorescence labeling was performed in neural tissue using UCH L1 antibody and polyclonal Ub antibody that predominantly recognizes free Ub (Sigma) (15). It was found that immunoreactivities to anti-UCH L1 and anti-Ub colocalized within the neuron (Fig. 2B, upper panel). Moreover, Ub immunoreactivity was reduced in neurons in *gad* mice (Fig. 2B, lower panel). In the peripheral nerve, neuronal axons are enwrapped by myelin of glial schwann cells that are immunoreactive to myelin basic protein antibody (Fig. 2C, right and left panels). Immunohistochemisty

Downloaded from https://academic.oup.com/hmg/article/12/16/1945/2355580 by guest on 20 August 2022

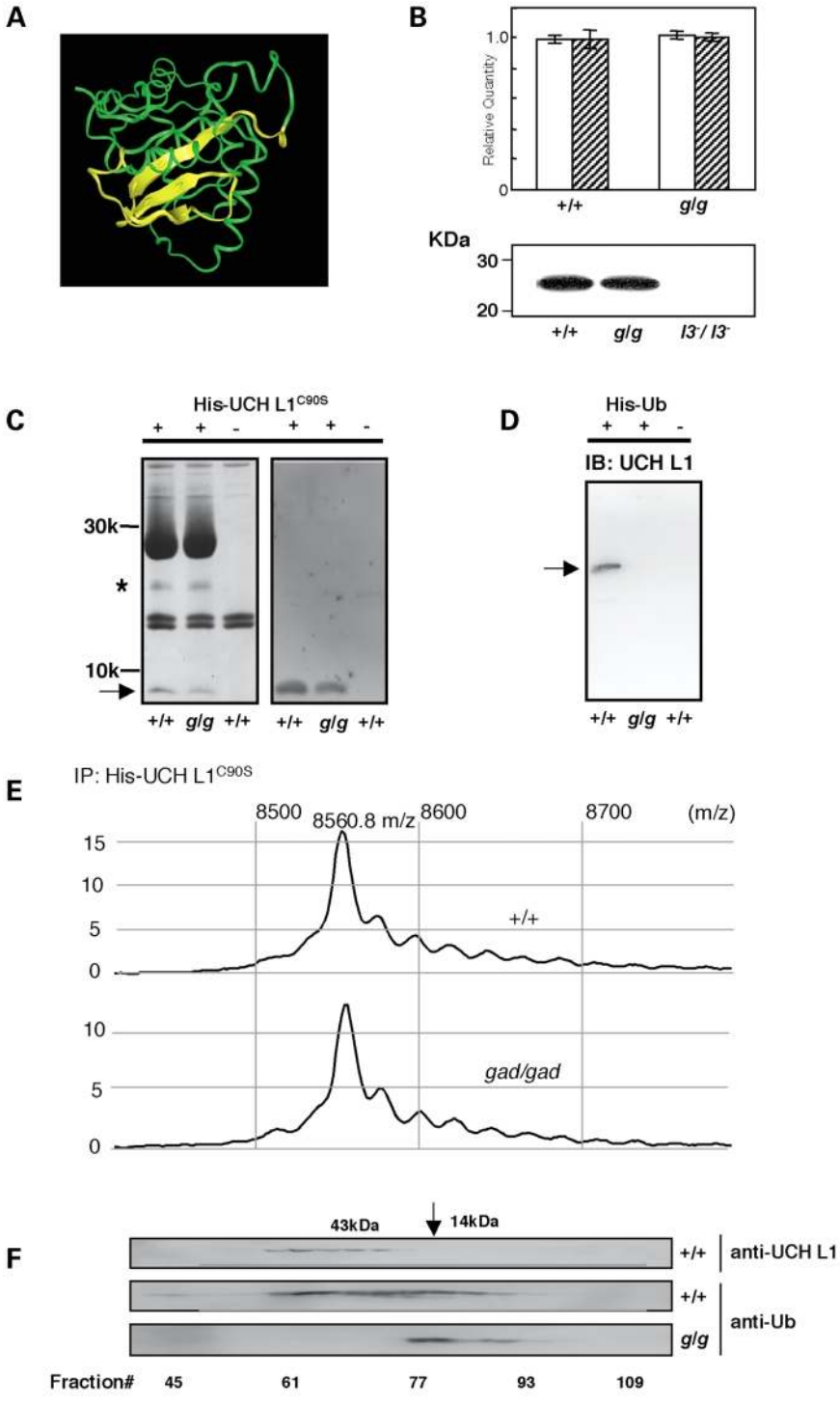

Figure 1. UCH L1 associates with ubiquitin. (**A**) Mouse UCH L1 was modeled after the crystal structure of human UCH L3 (14) using Insight II/Modeler (SGI). Secondary structures of the peptides deleted in the gracile axonal dystrophy (*gad*) mouse are shown in yellow. (**B**, upper panel) Quantitative RT–PCR for *Uch l3* was performed using total RNA from wild-type and *gad* (*gad/gad*) cerebra ($n = 3$ each). Mean values are shown with SEM. β-Actin (open bar) or GAPDH (solid bar) were used as internal controls. (B, lower panel) Soluble fractions (20 μg) of wild-type (+/+), the *gad* (g/g) and *Uch* $l3^{\Delta 3\text{-}7}$/*Uch* $l3^{\Delta 3\text{-}7}$($l3^{-}$/$l3^{-}$) (38) mouse brains were subjected to SDS–PAGE and immunoblotted with anti-UCH L1. (**C**) Eluates from pull-down assays using His-UCH $L1^{C90S}$ and brain lysate were subjected to SDS–PAGE, stained with Coomassie brilliant blue (left panel) and the band intensities to mono-Ub were compared. Eluates were also immunoblotted with monoclonal anti-Ub (right panel; Chemicon). Arrow shows the bands corresponding to mono-Ub. Asterisk shows the non-specific band that is co-purified during UCH L1 purification. (**D**) Eluates from pull-down assays using His-Ub and brain lysate were subjected to SDS–PAGE and immunoblotted with anti-UCH L1. The arrow shows the band corresponding to UCH L1. (**E**) Eluates from pull-down assays using His-UCH $L1^{C90S}$ and brain lysate were desalted with a C_{18} zip tip column and subjected to SELDI analysis. An m/z range near that expected for Ub ($m/z = 8562$) is presented. (**F**) Selected gel filtration chromatography fractions from wild-type brain lysates (upper and middle panels) and *gad* mice brain lysates (lower panel) were subjected to SDS–PAGE and immunoblotted with anti-UCH L1 (upper panel) or anti-Ub (middle and lower panels). The arrowhead and arrow correspond to the peak ovalbumin (43 kDa) and ribonuclease A (14 kDa) fractions, respectively.

Downloaded from https://academic.oup.com/hmg/article/12/16/1945/2355580 by guest on 20 August 2022

Table 1. Kinetic parameters for hydrolysis of ubiquitin-7 amid-4 methyl-coumarin (Ub-AMC) by mouse UCH L1 and inhibition by Ub

Enzyme	K_m (μM)	k_{cat} (s^{-1})	$10^6 \times k_{cat}/K_m$ ($M^{-1}\,s^{-1}$)	K_i (μM)
UCH L1^{WT}	0.16	0.02	0.13	3.3
UCH L1^{D30K}	—	0	0	[0.28][b]
UCH L1^{C90S}	—	0[a]	0	[0.86][b]

Steady-state kinetic parameters were determined at 25°C in assay buffer.
The mean values of three independent experiments are shown.
[a]No products were observed after 30 min with 5 mM enzyme.
Inhibitions were not assayed due to the lack of activity to substrates.
[b][Ratio of pulled down Ub to WT].

shows Ub immunoreactivity is decreased in neurons but not at glial schwann cells (Fig. 2D, middle panel).

Subsequently, cytosolic fractions of various nervous tissues that include both neuron and glia were subjected to SDS–PAGE and immunoblotted with a monoclonal Ub antibody that recognizes both free and conjugated Ub in denatured states (Chemicon) (15). The principal band corresponded to free mono-Ub, the intensity of which was reduced in *gad* mouse tissues (Fig. 3A, right panel) suggesting that mono-Ub is decreased in the absence of UCH L1 in the nervous system. A longer exposure or autoclaving the membrane enhanced the bands corresponding to Ub conjugates where no significant differences between wild-type and *gad* mice were observed (data not shown). Then mono-Ub levels in the nervous systems in <2-week-old wild-type and *gad* mice were measured by the radioimmunoassay (13). The inhibition rates for the ^{125}I-mono-Ub bound to antibody US-1 by brain lysates were compared with the standard curve generated by unlabeled mono-Ub (13). US-1 is specific antibody for free mono-Ub (13). Reduced levels of free mono-Ub (~20–30% reduction) were observed in each of the *gad* mouse tissues even at this early age (Fig. 3B; pathology in these mice was apparent only after >6 weeks). Immunoblotting and radioimmunoassay use cell lysates that contain both neuron and glia, which appears to be the reason for the apparent discrepancy between the large difference in Ub immuno-histochemistry in neurons and relatively smaller differences in mono-Ub levels in immunoblotting/radioimmunoassay.

These data show that Ub is associated with UCH L1 in neurons. Absence of UCH L1 reduces the mono-Ub level in neurons, which causes the reduction of overall mono-Ub level in the nervous system.

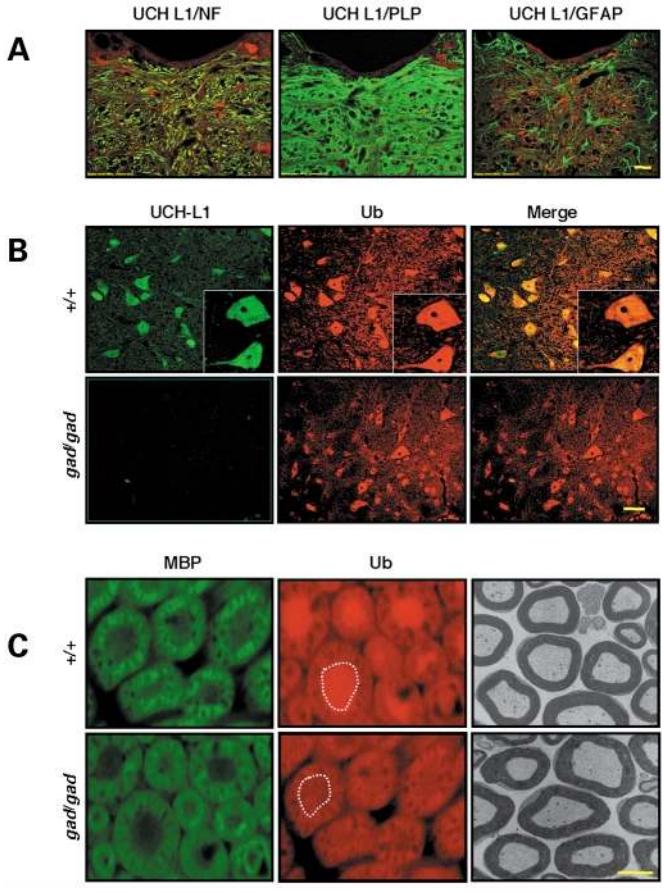

Figure 2. Loss of UCH L1 decreases ubiquitin immunoreactivity. Confocal laser scanning microscopy of mouse brain stem sections (**A**, **B**), sciatic nerve (**C**; left and middle panels) and electron microscopy for sciatic nerve (C; right panels) from 12-week-old wild-type or *gad* mice. (A) Immunohistochemistry to coronal sections at the brain stem, pons (fourth ventricule situates at the upper edges). Antibodies to a neuron marker, neurofilament (NF; left panel, green) and a glial oligodendrocytes marker, proteolipid protein (PLP; middle panel, green) and a glial astrocytes marker, glial fibrillary acidic protein (GFAP; right panel, green) were used for co-immunostaining with anti-UCH L1 (red). Immunoreactivity to anti-NF partially merges with that to anti-UCH L1. NFs exist at neuritis but not at a cell body of a neuron, whereas UCH L1 is expressed at both neuritis and cell bodies. Immunoreactivities to anti-PLP and anti-GFAP do not co-localize with that to anti-UCH L1. Scale bars, 40 μm. (B) Sections at neuronal nucleus in the pons from wild-type (upper panel) and *gad* mice (lower panel) were stained with anti-UCH L1 (green) and polyclonal anti-Ub (red; Sigma) on the same slide. Immunoreactivity to anti-UCH L1 is merged with that to anti-Ub. Moreover, immunoreactivity to anti-Ub is decreased in the *gad* mice that showed no reactivity to anti-UCH L1. Scale bars, 10 μm. Insets are images at four times higher magnification. (C) Sciatic nerve is composed of inner neuronal axon and outer myelin that is immunoreactive to anti-myelin basic protein (MBP, the marker of glial schwann cells, left panels). Immunoreactivity to anti-Ub in the neuronal axon (inside of dashed line) is decreased in the *gad* mouse, whereas the immunoreactivity to anti-Ub in glial myelin (outside the dashed line) is comparable between wild-type and *gad* mice. Electron microscopic images show fine structures of myelin and axon that are similar between wild-type and *gad* mouse in this 12 weeks of age (right panel). Scale bars, 10 μm.

UCH L1 overexpression increases Ub levels

The effect of UCH L1 overexpression on Ub levels was examined in both cultured cells and transgenic mice. Adenovirus vectors expressing UCH L1 (adeno-*Uch l1*) or β-galactosidase (adeno-β-*gal*) were transfected into mouse embryonic fibroblasts (MEF) cells that do not express UCH L1. After transfection, UCH L1 was induced by Cre recombinase. Reactivitiy to anti-Ub exist at both nucleus and cytosol in adeno β-*gal* transfected and non-transfected MEF cells (Fig. 4B and C). Surprisingly, MEF cells transfected with adeno-*Uch l1* express UCH L1 dominantly at cytosol, where immunoreactivities to anti-Ub and anti-UCH L1 are completely merged (Fig. 4A). Then the levels of Ub were compared by immnoblotting. The level of free mono-Ub as well as ubiquitylated proteins increased relative to the β-*gal* control at 24 h after UCH L1 induction (Fig. 4D; band intensity ratio of

Downloaded from https://academic.oup.com/hmg/article/12/16/1945/2355580 by guest on 20 August 2022

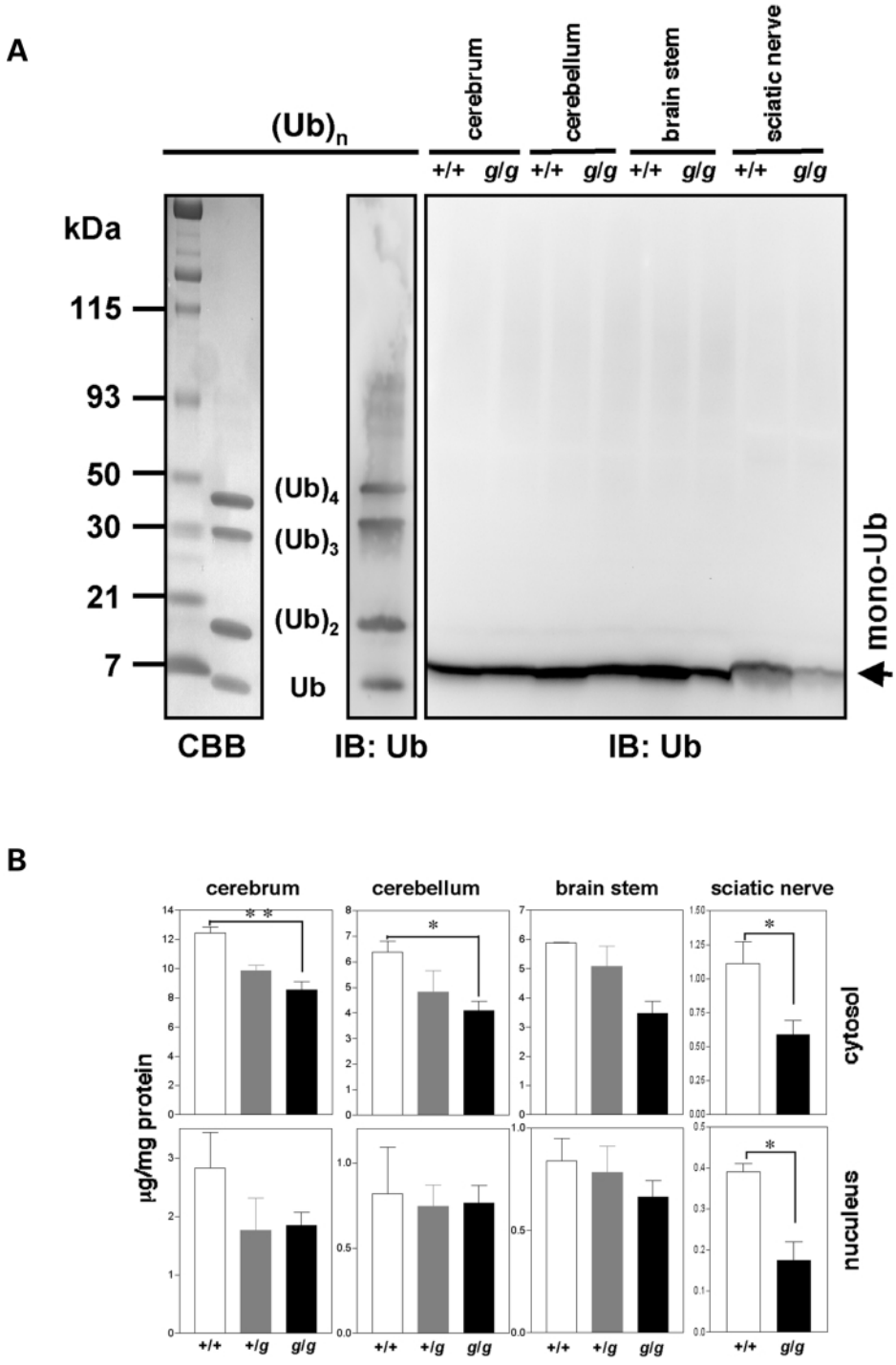

Figure 3. Loss of UCH L1 decreases the level of monoubiquitin. (**A**) A mixture of 1 μg ubiquitin and 4 μg poly-Ub was subjected to SDS–PAGE and stained with coomassie brilliant blue (left panel). Ten percent of this mixture was electrophoresed and immunoblotted with a monoclonal antibody to Ub (Chemicon) that recognizes both conjugated and unconjugated mono-/poly-Ub in denatured states (middle panel). Cytosolic fractions (20 μg) from various neuronal tissues of wild-type and *gad* mice were immunoblotted using the same antibody (right panel). (**B**) Levels of free mono-Ub in cytosolic (upper) and the nuclear (lower) fractions were measured by radioimmunoassay (16) in various brain structures from mice less than 2 weeks old ($n = 5$ for cerebrum, cerebellum and brain stem; $n = 4$ for sciatic nerve). Mean values with SEM are shown as open (+/+), gray (+/−) or black (*g*/*g*) bars. $^{**}P < 0.01$; $^{*}P < 0.05$.

adeno-*Uch l1* transfected cell to β-*gal*-transfected cell were 2.3 ± 0.2 to bands corresponding to mono-Ub and 1.5 ± 0.2 to bands corresponding to MW50-115; $n = 3$, corrected by β-actin).

Next, mice carrying a *Uch l1* transgene under control of the EF-1α promoter were generated (Fig. 5A). These mice exhibit no apparent neurological phenotype during life. However, transgenic (Tg) mouse expressing a high copy number of

Downloaded from https://academic.oup.com/hmg/article/12/16/1945/2355580 by guest on 20 August 2022

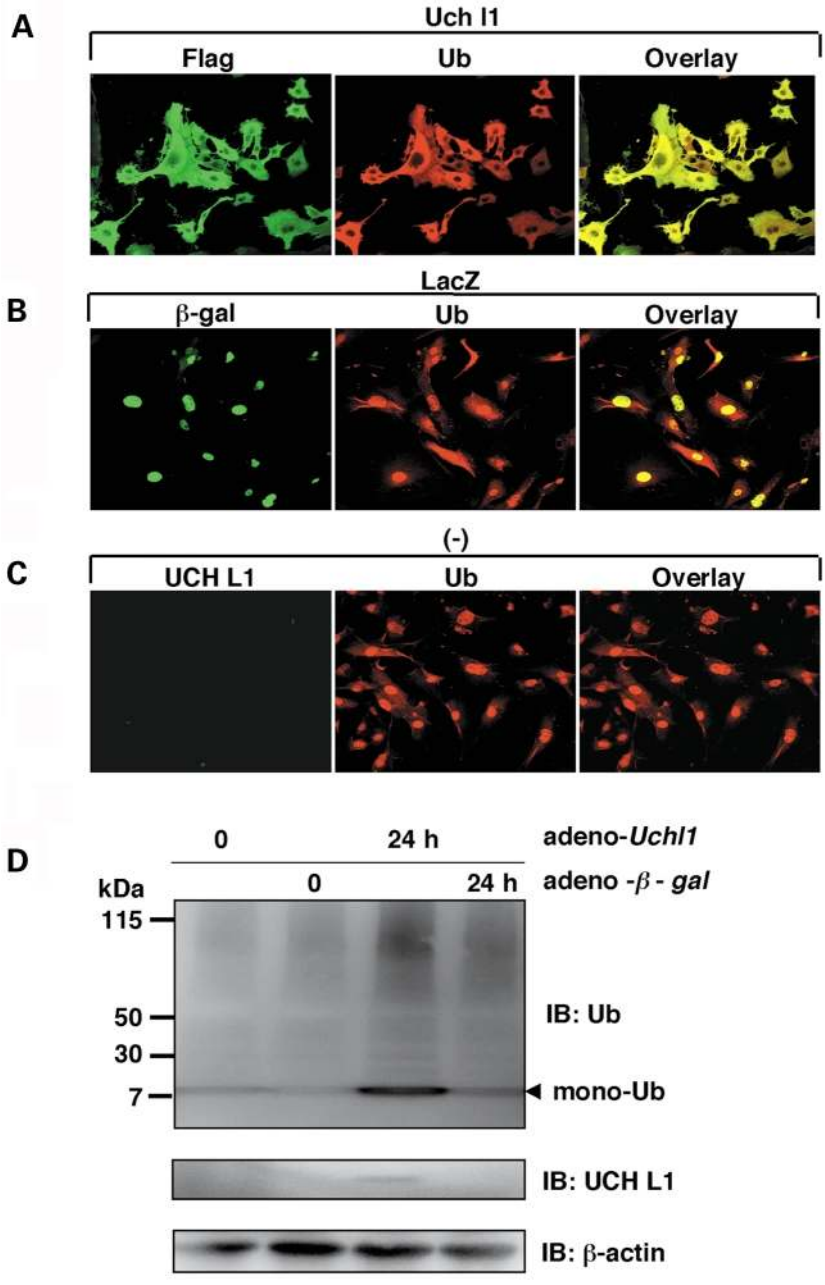

Figure 4. Overexpressed UCH L1 co-localizes with ubiquitin and increases ubiquitin levels in cultured cells. (**A**–**C**) E13.5 primary mouse embryonic fibroblasts (MEF) cells were transfected with adenovirus vectors expressing either *Uch l1* (A) or β-gal (B) or not transfected (C). UCH L1 was induced using Cre recombinase for 24 h. Antibodies to flag-tag and β-gal were used for immunostaining to exogenic UCH L1 and β-gal (A, B; left panels). An absence of immunoreactivity to anti-UCH L1 showed the lack of endogenous UCH L1 expression in MEF cells (C; left panel). MEF cells were also labeled with polyclonal anti-Ub (Sigma; A–C; middle panels). Immunoreactivities to anti-Ub/-UCH L1 completely merge in MEF cells transfected with adeno-*Uch l1* (A; right panel), but not in cells transfected with β-gal (B; right panel) and not transfected (C; right panel). Ub localization appears to be recruited to the UCH L1. (**D**) Cell lysates were immunoblotted with anti-Ub (Chemicon) or anti-UCH L1 at the indicated times (upper and middle panels). The same membrane was re-blotted with an antibody to β-actin (lower panel). Band intensities were measured at the bands corresponding to mono-Ub and poly-ubiquitinated bands at MW50-115 kDa and normalized by β-actin intensities.

foreign DNA and high-level of mRNA from *Uch l1* transgene were all infertile ($n = 6$, manuscript in preparation). Therefore, we examined two of these infertile Tg mice, 11 and 22 (Fig. 5B). Immunohistochemistry of brain sections showed increased levels of UCH L1 immunoreactivity in the nervous system of Tg mice (Fig. 5C; left panel, cerebral cortex; right panel, cerebellum). The antibody to Ub that preferentially stains free mono-Ub showed a significant increase in Ub immunoreactivity in Tg mice (Fig. 5D; cerebellum). Immunoblotting also showed the increased level of mono-Ub in Tg mice (Fig. 5E; band intensity for mono-Ub of Tg 22 to wild-type was 2.3 in cerebrum and 1.5 in cerebellum). These data show that UCH L1 overexpression increases the level of mono-Ub in the cultured cells and nervous system *in vivo.*

Downloaded from https://academic.oup.com/hmg/article/12/16/1945/2355580 by guest on 20 August 2022

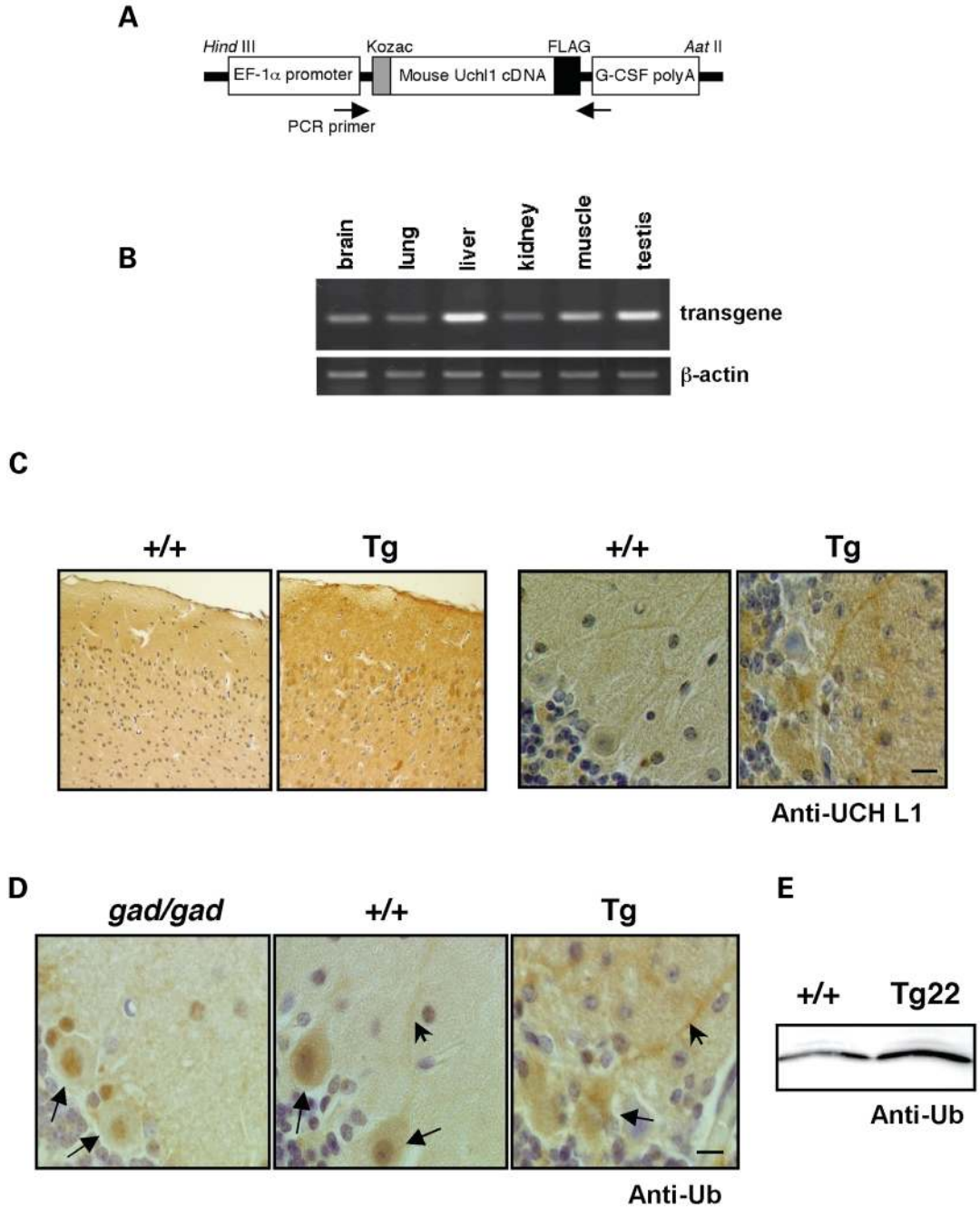

Figure 5. UCH L1 overexpression increases ubiquitin level in the mouse nervous system. (**A**) Construction of the transgenic vector. Flag-tagged mouse *Uch l1* cDNA was subcloned into pEF-Bos vector that carries EF-1α promoter. (**B**) Total RNAs of 5 μg from various organs of transgenic (Tg) mouse 22 were subjected to RT–PCR using specific primers to transgenic *Uch l1* cDNA (upper panel) and β-actin (lower panel). (**C**) Immunohistochemisty to anti-UCH L1 antibody to cerebral cortex (left panels) and cerebellum (right panels) from Tg 22 and wild-type mouse. Scale bars, 20 μm. (**D**) Cerebellar sections from *gad* (*gad/gad*), wild-type (+/+), and UCH L1 transgenic mice (Tg 22) brains were analyzed by immunohistochemistry using polyclonal anti-Ub (Sigma) as the primary antibody. Ub reactivity was increased in Tg 22 mouse. The *gad* mouse showed decreased immunoreactivity to anti-Ub. Arrows and arrowheads indicate Purkinje cell body and neurites, respectively. Scale bars, 20 μm. Twenty micrograms of proteins of the cerebrum (**E**) and cerebellum from Tg 22 and wild-type mouse were subjected to SDS–PAGE and immunoblotted with anti-Ub.

Mechanism by which UCH L1 increases Ub levels

The basis of the UCH L1-mediated increase in Ub levels was examined using three different approaches. First, Ub transcriptional regulation was examined in both wild-type and *gad* mice. The mRNA levels of all four Ub genes, *Uba52*, *s27a*, *UbB* and *UbC*, were analyzed by quantitative PCR but no significant differences were observed between wild-type and *gad* mice (Fig. 6A). A reporter assay using the *UbC* gene promoter also showed no effect of UCH L1 on

Downloaded from https://academic.oup.com/hmg/article/12/16/1945/2355580 by guest on 20 August 2022

transcriptional activation of the *UbC* gene (Fig. 6B). These experiments showed that UCH L1 does not upregulate Ub levels via transcriptional activation.

Second, to address the possibility that a reduction in the release of mono-Ub from poly-Ub or Ub-conjugated proteins affects the level of free mono-Ub in *gad* mice, UCH L1-catalyzed release of mono-Ub from substrates was tested. UCHs can generate mono-Ub from poly-Ub and peptide–ubiquityl amides *in vitro* (12). However, no enhanced intensity corresponding to the release of Ub from poly-Ub (Fig. 3A; compare left and right panels) or mass spectra corresponding to the hydrolysis of peptide–ubiquityl amides (Fig. 1E) was observed in the *gad* mouse immunoprecipitates from brain lysates. Alternatively, an unknown substrate could be upregulated as poly-Ub-conjugated proteins (multi-Ub) in *gad* mice. Therefore, multi-Ub levels were measured in soluble mouse brain lysates by sandwich ELISA using antibody FK2 that is specific for multi-Ub (16–18) (Fig. 6C). No difference in the level of multi-Ub was observed between the wild-type and the *gad* mouse at less than 2 weeks of age. These data argue against the hypothesis that the deficiency in UCH L1-catalyzed release of mono-Ub from multi-Ub is responsible for the decreased level of Ub observed in the *gad* mouse.

Third, the effect of UCH L1 expression on Ub metabolism was examined in MEF cells transfected with either adeno-*Uch l1* or -β-*gal*. Mono-Ub levels were monitored for 30 h after pulse-chase labeling and Ub degradation was compared by autoradiography. Ub half-life was extended in MEF cells transfected with UCH L1 (Fig. 6D). Since lysosomes are implicated as the site of Ub degradation, we examined the effect of the lysosomal inhibitor EST (2,3-*trans*-epoxysuccinyl-L-leucylamide-3-methyl butane ethyl ester) on Ub metabolism (19,20). EST extended Ub half-life in both adeno-*Uch l1*- and adeno-β-*gal*-transfected MEF cells (Fig. 6D) and, under these conditions, mono-Ub degradation was comparable between the adeno-*Uch l1*-transfected cells and the control cells (Fig. 6D).

These data suggest that UCH L1 affects Ub degradation and alters its metabolism, and that Ub degradation occurs in lysosomes.

UCH L1 affinity for Ub appears to be indispensable for the maintenance of Ub levels

To further clarify the effect of UCH L1 on Ub levels, his-tagged *Uch l1* and mutants were transfected into dopamine-producing SH-SY5Y neuronal cells (Fig. 7). UCH L1 and Ub were then visualized using confocal immunofluorescence microscopy. Cells transfected with wild-type *Uch l1* showed a relative increase in Ub immunoreactivity compared with mock-transfected cells (anti-Ub; Sigma, polyclonal; Fig. 7A and E) consistent with Ub upregulation by UCH L1. *Uch l1*^{I93M}, implicated in the pathogenesis of PD, also increased Ub immunoreactivity comparable to wild-type *Uch l1* (Fig. 7B and E). Increased Ub immunoreactivity was also evident in cells transfected with *Uch l1*^{C90S}, which retains Ub binding affinity but lacks C-terminal hydrolase activity (Fig. 7C and E; Table 1) (9). However, significant increase in Ub immunoreactivity was not observed with mutant *Uch l1*^{D30K} (Fig. 7D and E), which carries a charge reversal on the surface of the protein that is presumed to interact with cationic residue of Ub (21). This mutant protein exhibits markedly lower affinity for Ub and has no hydrolase activity (Table 1). These data suggest that UCH L1-mediated increases in Ub levels are a function of UCH L1 affinity for Ub rather than hydrolase activity.

DISCUSSION

In spite of the abundance of UCH L1 in the nervous system and its importance in the neurodegenerative diseases, the *in vivo* functions of UCH L1 have been remained unknown (6–13). The *gad* mouse and the UCH L1 transgenic mouse revealed a novel role for UCH L1 in neurons. Our data indicate that UCH L1 is associated with mono-Ub and elevates the level of mono-Ub in neuron. Previously, Doa4, a deubiquitinating enzyme belonging to UBPs, was reported to elevate the level of Ub in yeast, although the association of Doa4 with Ub was not mentioned (19). From a genetic complementation study, Doa4 was inferred to be involved in endosomal–lysosomal pathway (20). Our pulse-chase labeling using MEF cells suggests that UCH L1 affects Ub metabolism and extends its half-life by inhibiting Ub degradation. As an inhibitor of lysosomal function extended Ub half-life and partially diminished the effect of UCH L1, UCH L1 probably prevents Ub degradation in lysosomes. Thus, our results also suggest the link of DUBs to the endosome–lysomal pathway. Recently, it was demonstrated that Ub itself contains all the necessary signals for both targeting and degradation of monoubiquitylated proteins in the endosomal–lysosomal pathway, with the crucial Ub residues being Gln2, Phe4, Lys6, Leu8, Val26, Leu43, Ile44, Glu64 and Val70 (22,23). Possibly some fraction of free Ub itself is shunted into the endosome–lysosomal pathway and UCH L1 binding to Ub may suppress this route by masking Ub residues that are requisite for targeting. Alternatively, it may be possible that UCH L1 deubiquitylates ubiquitylated proteins before degradation within the endosome–lysosome pathway. However, UCH L1^{C90S}, lacking hydrolase activity, still retains the ability to maintain Ub levels, suggesting that physical association with UCH L1 rather than its deubiquitylating activity promotes Ub stability. Although UCH L1 can very slowly cleave poly-Ub and Ub-small molecule adducts *in vitro* (4), we did not find accumulation of such Ub species in *gad* mice. This finding may reflect functional redundancy between UCHs and UBPs. Alternatively, such Ub species may be detergent insoluble and exist within aggregates of Ub in dot-like structures observed in *gad* mice (10).

It has been long known that Ub-containing protein aggregates as hallmarks of various neurodegenerative conditions (2). Such aggregates are remnants of inadequate proteolysis and suggest either surpluses of aggregation-prone abnormal proteins or insufficiencies in Ub-dependent proteolysis (Fig. 8). PD caused by A53T and A30P mutations of α-synuclein appear to be the examples for the former case. These mutant proteins are more stable than wild-type and presumed to surpass the critical concentration of α-synuclein for oligomerization (24,25). The latter case appears to account for both a *Uch l1* gene deletion in the *gad* mouse and the parkin gene mutations in the patients with PD. Loss of function mutations in Parkin E3 ligase may prevent this enzyme from properly ubiquitylating putative

Downloaded from https://academic.oup.com/hmg/article/12/16/1945/2355580 by guest on 20 August 2022

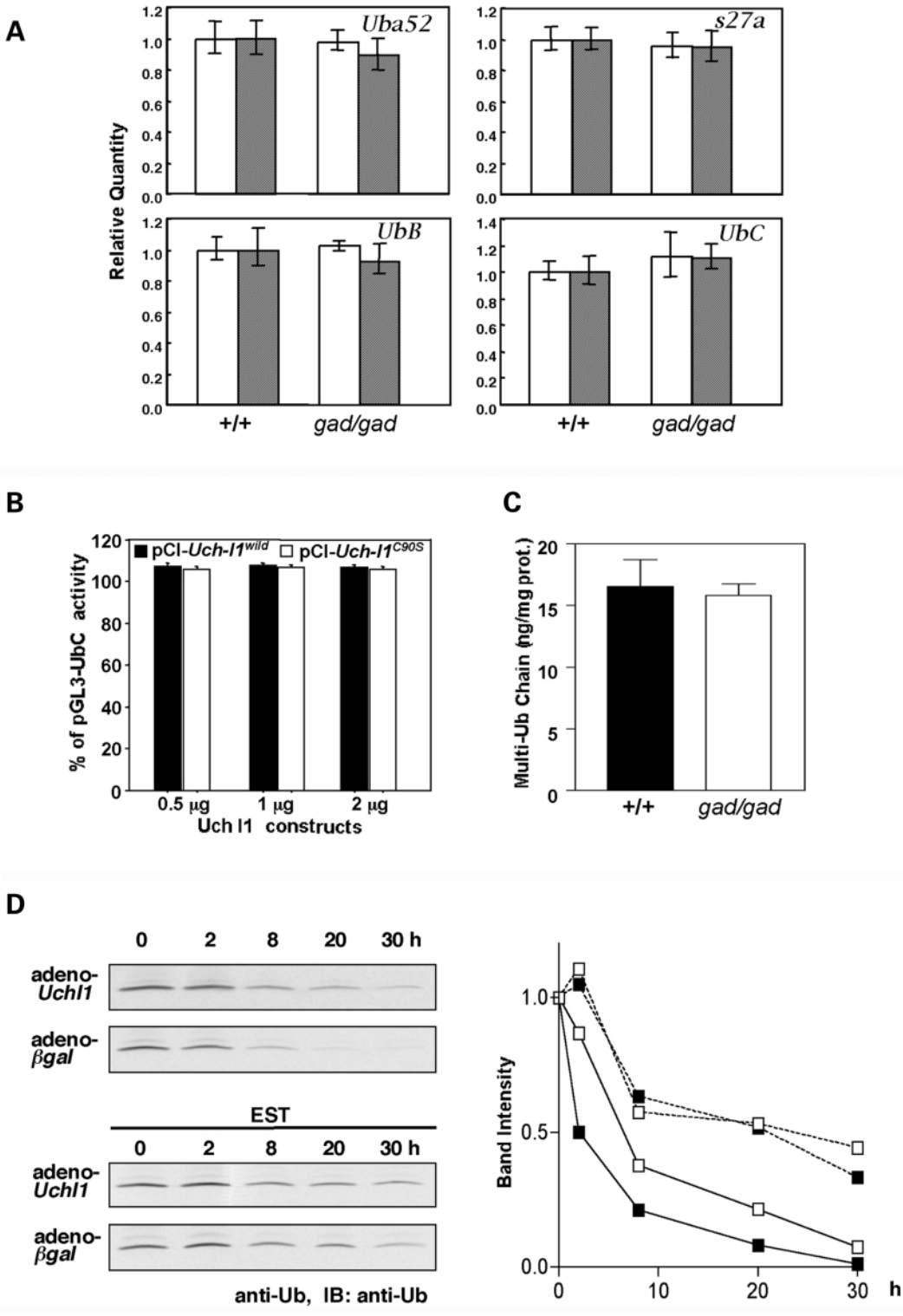

Figure 6. Effects of UCH L1 on transcription, processing and post-translational state of ubiquitin. (**A**) Quantitative RT–PCR for *Uba52*, *s27a*, *UbB* and *UbC* was performed using total RNA from wild-type and *gad* (*gad/gad*) cerebrum ($n = 3$). Mean values are shown with SEM. β-Actin (open bar) or GAPDH (solid bar) were used as internal controls. (**B**) Dual luciferase assay of a vector containing the +18 to +1227 bp region of the human Ub C promoter (pGL3-*UbC*) co-transfected with either UCH L1 (pCI-neo-$Uchl1^{WT}$; solid bar) or an active site mutant of UCH L1 (pCI-neo-$Uchl1^{C90S}$; open bar). Mean values from eight independent experiments are shown with SEM. (**C**) Levels of multi-Ub chain (conjugated poly-Ub) in cerebellum cytosolic fractions were measured by ELISA from 2-week-old mice ($n = 6$) (16–18). Mean values with SEM are shown as filled (+/+) or open (*gad/gad*) bars. (**D**) Adeno-*Uchl1*-transfected or adeno-β-*gal*-transfected MEF cells were labeled with [^{35}S]-Met. Autoradiograms of anti-Ub immunoprecipitates pulse-chased at the indicated times in the absence (left upper panels) or presence of EST (2,3-*trans*-epoxysuccinyl-L-leucylamide-3-methyl butane ethyl ester; left lower panels) are shown. Relative band intensities are quantified and mean values of two independent experiments are shown (right).

Downloaded from https://academic.oup.com/hmg/article/12/16/1945/2355580 by guest on 20 August 2022

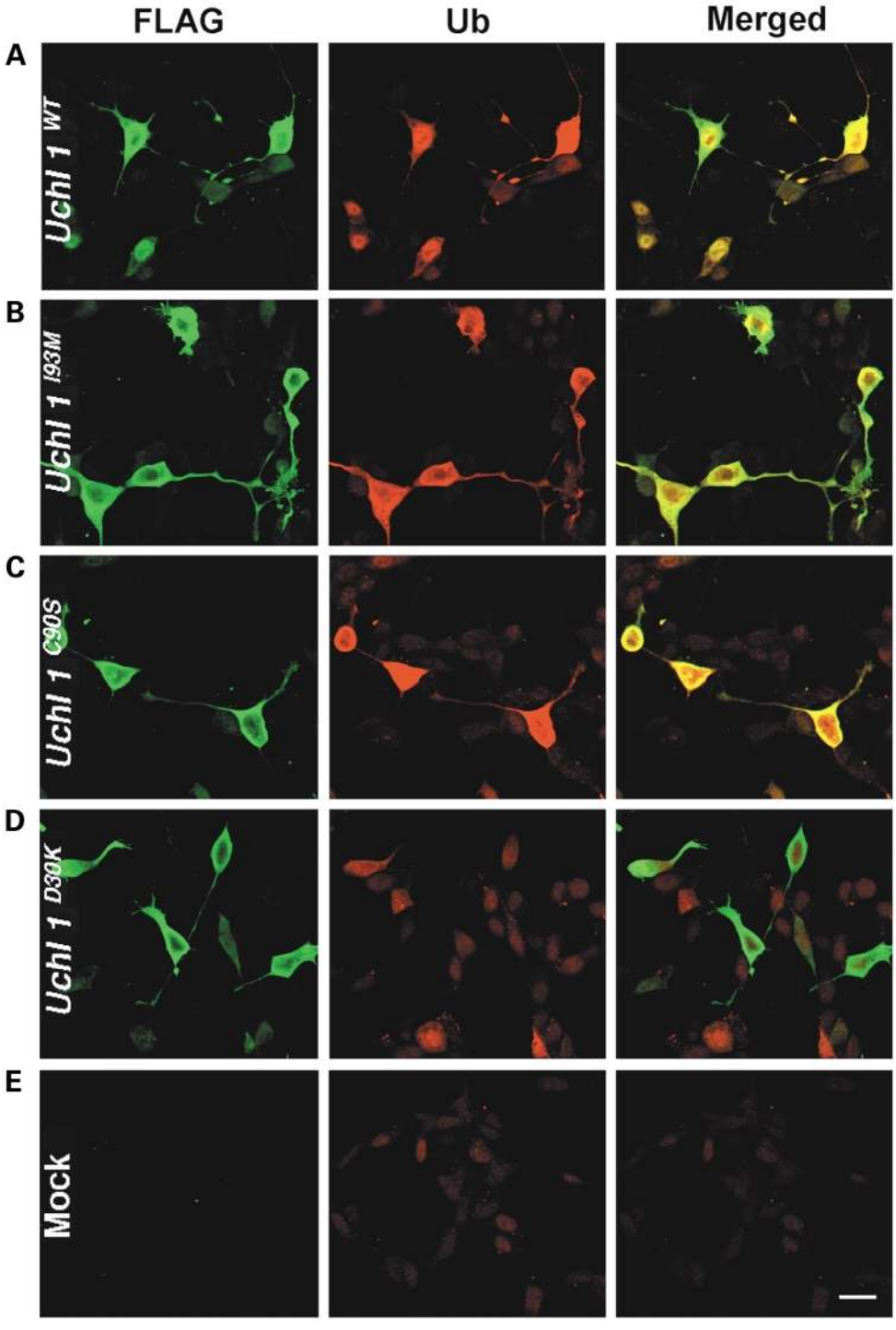

Figure 7. Effect of UCH L1 mutants on ubiquitin expression. Plasmids pcDNA3-*Uchl1*^{WT} (**A**), -*Uchl1*^{I93M} (**B**), -*Uchl1*^{C90S} (**C**), -*Uchl1*^{D30K} (**D**) and vector alone (**E**) were transfected into SH-SY5Y cells and expressed. Antibodies against flag-tag and Ub (Sigma, polyclonal) were used to detect transfected UCH and endogenous Ub, respectively. The faint green staining (left panels) reflects non-specific staining of cells that escaped transfection. Scale bars, 20 μm.

substrates (26,27), causing substrate accumulation and toxicity to neurons at the substantia nigra. Loss of functional UCH L1 could also lead to inadequate ubiquitylation via decrease of free Ub. An initial pathological lesion begins at the synapse of the sciatic nerve in the *gad* mouse. Ub is known to be transported over long distances via slow axonal transport to synapse (28). Ub decrease and the consequent inadequate ubiquitylation of proteins may trigger increased levels of proteins that should undergo Ub-dependent degradation, resulting in the accumulation of such proteins within spheroids observed in *gad* mice (11). The *gad* mouse phenotypes resemble those of Charcot–Marie–Tooth diseases (CMT) in humans. Although there are no

Downloaded from https://academic.oup.com/hmg/article/12/16/1945/2355580 by guest on 20 August 2022

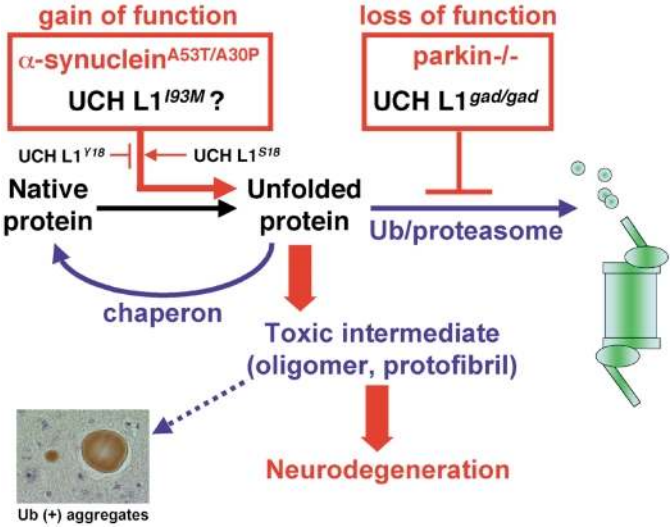

Figure 8. Common pathway of neurodegeneration. Unfolded proteins are refolded by molecular chaperons or degraded by the ubiquitin/proteasome pathway. The red boxes illustrate that excessive production of insoluble proteins by genetic defect (such as A53T/A30P mutations of α-synuclein in Parkinson's disease) or insufficiencies in the ubiquitin/proteasome pathway (such as *Uch l1* gene deletion in the *gad* mouse and the parkin gene mutations in the patients with PD) alter the proportion of denatured proteins within the cell. The accumulation of a toxic intermediate (oligomer or protofibril) is proposed to precede and promote neurodegeneration.

CMT or peripheral neuropathies that map to the proximity of the human *UCH L1* locus so far, immunohistological profiling of UCH L1 and Ub in peripheral nerves would be helpful in delineating a human *gad* analog.

Human *UCH L1* deletion mutants have not been reported although polymorphism and missense mutations of UCH genes are linked to PD (29–32). In idiopathic PD, particularly of Japanese or Chinese origin, UCH L1 gene polymorphism at position 18 is linked to a disease susceptibility (29–32). The S18Y mutation is common in Japanese and Chinese compared with Europeans and is reportedly protective for PD (19–32). Recently, UCH L1 was found to exhibit dimerization-dependent ubiquityl ligase activity at Lys63 of acceptor Ub molecules *in vitro* (13). Polyubiquitylated proteins linked to Lys48 of Ub are destined for proteasomal degradation, while those linked to Lys63 of Ub are stable. The protective variant Y18-UCH L1 exhibits diminished dimerization and ligase activities relative to S18-UCH L1, and therefore Y18-UCH L1 is predicted to accelerate degradation of proteins such as α-synuclein by making less stable species conjugated to Lys 63 of Ub. Thus, the decreased susceptibility to PD in individuals carrying the S18Y mutation could be explained by the low concentration of α-synuclein, which is yet confirmed *in vivo* (13) (Fig. 8). The I93M mutation in UCH L1 is reported in familial PD with dominant inheritance (9). α-Synuclein (dominant form) or the of parkin or DJ-1 (recessive forms) may also cause familial PD (33–35). The glycosylated form of α-synuclein is a substrate for parkin (36). Our present data indicate that UCH L1 upregulates Ub levels *in vivo*, and therefore UCH L1, parkin and α-synuclein appear to be interrelated with respect to Ub and ubiquitylation pathways. As with α-synuclein, the loss of UCH L1 function does not appear to cause PD (11,37). In patients carrying the UCH L1 mutation I93M, both ligase and hydrolase activities are presumed to be partially reduced (9,13). Our data show that UCH $L1^{I93M}$ enhances Ub immunoreactivity similar to UCH $L1^{WT}$ in transfected cells. Moreover, we did not find evidence for nigrostriatal dopaminergic pathology in either *gad* mouse heterozygotes or homozygotes. Therefore, an as yet unknown 'gain of toxic function' condition may underlie PD in patients carrying UCH $L1^{I93M}$ (Fig. 8).

Our results reveal that the fundamental defects in the *gad* mouse are due to a lack of UCH L1 and consequent Ub decrease. Ub and Ub-dependent proteolysis are involved in nearly all cellular processes and therefore it is likely that *gad* mice exhibit a wide variety of neuronal malfunctions that are not recognized by routine histology. Thus, in light of our present data we are currently re-evaluating *gad* mouse phenotypes including behavior, neuronal regeneration and apoptosis. These studies will broaden our understanding of the role of Ub pathways in neuronal function and neurodegenerative disorders.

MATERIALS AND METHODS

Plasmid and protein purification

Sequences encoding UCH L1 were amplified from a mouse brain cDNA library by polymerase chain reaction (PCR), and subcloned into either pQE-30 (Qiagen, Valencia, CA, USA) or pcDNA3 (Invitrogen, Groningen, The Netherlands) for expression in *E. coli* (for protein purification) or mammalian cells (for transfection), respectively. cDNA encoding UCH $L1^{gad}$ was obtained from a *gad* mouse brain by PCR. Another UCH L1 mutations were introduced by PCR-based site-directed mutagenesis (QuickChange Site-Directed Mutagenesis Kit, Stratagene, La Jolla, CA, USA) of template plasmids using primers designed to introduce specific mutations (D30K, C90S, I93M). Proteins overexpressed in *E. coli* were purified using Ni-agarose (Qiagen) as per the manufacturer's protocol and purified further by gel filtration using a Hi Load™ 16/60 Superdex 75 column (Amersham Pharmacia, Uppsala, Sweden).

Generation of adeno-vectors, antibodies and Ub level determination

Recombinant plasmids containing adeno-*Uch l1* and -β-*gal* were constructed using the Adenovirus Expression Vector Kit as per the manufacturer's instructions (Takara, Tokushima, Japan). Briefly, *Uch l1-flag* and β-*gal-flag* genes were inserted individually into the cosmid vector pAxCANLw containing the CAG promoter, the stuffer sequence and two loxP sequences. These recombinant cosmids were co-transfected into HEK 293 cells with a restriction enzyme-digested adenovirus DNA-TPC to generate a recombinant adenovirus through homologous recombination. Expression of the *Uch l1*- or β-*gal*-gene is achieved by removal of the stuffer sequence between the loxP sequences by Cre recombinase (expressed by co-transfection with pAx CANCre DNA).

Downloaded from https://academic.oup.com/hmg/article/12/16/1945/2355580 by guest on 20 August 2022

Immunizing with different ubiquitin-carrier conjugates produced five antibodies and, among them, US-1 was found to be specifically reactive to mono-Ub (16). Immune complexes of US-1 and ^{125}I-mono-Ub were obtained by centrifuge and counted in a gamma counter. The inhibition for the tracer bound to the antibody in the presence of lysates was measured and mono-Ub level was determined from the standard curve generated by unlabeled Ub (16). Monoclonal antibody FK2 that recognizes conjugated-multi-ubiquitin chain was used for immunoassay (sandwich ELISA) for multi-ubiquitin chains as described (17,18). This ELISA system shows an only negligible reactivity to free-Ub (17).

Fractionation, immunoaffinity purification and immunoblotting

Mouse brains were homogenized in lysis buffer (50 mM NaH_2PO_4/300 mM NaCl/10 mM imidazole, containing a complete protease inhibitor cocktail, pH 8.0) and centrifuged at 70 000*g* for 1 h to yield a cytosolic fraction. The nuclear fraction was extracted with lysis buffer containing 10% NP-40 and 400 mM NaCl. Insoluble materials were dissolved with 8 M urea. For pull-down assays, 200 µg of His_6-tagged UCH $L1^{WT, C90S, D30K}$ and 40 µl of Ni-NTA Agarose (Qiagen) were added to 750 µl mouse brain lysate containing 6 mg total protein. After gentle rotation overnight at 4°C, the Ni-NTA beads were washed three times with 200 µl of wash buffer (50 mM NaH_2PO_4/300 mM NaCl/20 mM imidazole, pH 8.0). The beads were eluted with 3 × 40 µl elution buffer (50 mM NaH_2PO_4/300 mM NaCl/250 mM imidazole, pH 8.0) and subjected to SDS–PAGE, stained with Coomassie brilliant blue (CBB) or immunoblotted. Densitiometric analysises were done using software PD QUEST (BioRad). For TOF analysis, 1 µl samples were spotted onto H4 hydrophobic-coated Protein Chip Array (Ciphergen Biosystems, Palo Alto, CA, USA) after desalting with a C_{18} zip tip column. The ionized proteins were detected and accurate mass was determined based on TOF analysis. TOF mass spectra were collected in the positive ion mode and signal averages of 50 laser shots were used to generate each spectrum. After SDS–PAGE on a 10–20% gradient gel, protein bands migrating at ~8 kDa were excised and digested within the gel with trypsin (Sigma). Digested peptide samples were then introduced via nano-spray into a QSTAR Pulsar LC/MS/MS system (Applied Biosystems, Foster City, CA, USA). Immunoblotting was performed as described (10) using antibodies to Ub (1 : 100, Chemicon, MAB1510) and UCH L1 (1 : 1000, Chemicon, polyclonal). The Ub antibody MAB1510 is reactive to both free and conjugated forms of Ub in immunoblotting (15). The epitopes of UCH L1 antibody were confirmed to recognize the region encoded by other than exons 7 and 8 of *Uch l1* gene, by using UCH $L1^{gad}$ protein produced by *E. coli* expression system. Ub and $(Ub)_n$ were purchased from Boston Biochem, MA, USA.

Immunohistochemistry, immunofluorescence and electron microscopy

Twelve-week-old mouse brain and sciatic nerve sections were analyzed by immunocytochemistry as previously described (10) using antibodies to Ub that is predominantly reactive to free Ub in immuno-histochemistry (1 : 100, Sigma) and UCH-L1 (1 : 40, Medac; monoclonal). Antibodies to neurofilament-M (NF; 1 : 200, Chemicon, monoclonal), glial fibrillary acidic protein (GFAP; 1 : 200, Chemicon, monoclonal), proteolipid protein (PLP; 1 : 200, Chemicon, monoclonal) and myelin basic protein (MBP; 1 : 200, QED bioscience, monoclonal) were used as neuronal, astrocytes, oligodendrocytes, schwann cell markers, individually. For immunofluorescence studies, anti-mouse-Cy3 or -FITC or anti-rabbit-conjugated-Cy3 or -FITC (1 : 500, Jackson Immuno Research) were used as secondary antibodies. MEF cells and SH-SY5Y cells were analyzed by immunofluorescence using either anti-flag tag (1 : 200, Sigma) or anti-Ub (1 : 100, Sigma) as the primary antibodies. Ultrastrucal studies by electron microscopy were performed as described using sciatic nerve (11).

Quantitative RT–PCR analysis and dual luciferase assays

Primers for the mouse *Uch l3* and four ubiquitin genes were designed and comparative reverse transcription–PCR (RT–PCR) was performed using Taq Man probe with the ABI PRISM 7700 (Applied Biosystems) using total RNA from wild-type and *gad* mouse brain ($n = 3$). The dual luciferase assay was performed using the +18 to +1227 bp region of the human Ub C promoter generated from human genomic DNA as per the manufacturer's instructions (Promega).

Pulse chase analysis

Transfected MEF cells were washed and incubated with methionine-free medium for 1 h. The cells were then pulsed with 200 µCi/ml [^{35}S]-Met (NEN) for 1 h and then washed and chased with 30 mM methionine for 30 h. At 0, 2, 8, 20 and 30 h the cells were harvested for immunoprecipitation with anti-Ub. Following SDS–PAGE on a 15% gel, radioactive bands were detected using the image analysis software PD QUEST (BioRad).

Transgenic UCH L1 mouse

Flag tagged mouse UCH L1 was subcloned into pEF-Bos vector under the strong promoter EF-1α. This plasmid was linearized by digestion with *Hind*III/*Aat*II, gel-purified and extracted twice with phenol/chloroform. A 2 µg/ml solution of linearized plasmid was used for pronuclear microinjection. Offspring were screened for the presence of the transgene by PCR of tail DNA. Expression of transgenic *Uch l1* mRNA was confirmed by reverse transcription of total RNA (5 µg) and subsequent PCR using specific primers (Fig. 5A). Primers to β-actin were used for internal controls.

Molecular simulation

Mouse UCH L1 was automatically modeled using Modeler software with Insight (MSI) interface. Briefly, mouse UCH L1 was modeled after the data from the crystal structure of human UCH L3 using the ClustralW algorithm. Human UCH L3 was used to derive spatial restraints expressed as probability density functions (14). These functions are used to constrain C^{α}–C^{α} distances, main chain N–O distances, main chain and side chain dihedral angles, etc. The individual constraints were assembled

Downloaded from https://academic.oup.com/hmg/article/12/16/1945/2355580 by guest on 20 August 2022

into a single molecular probability density function (MPDF). The three-dimensional protein model was then obtained by optimizing this MPDF. The optimization procedure itself employed a variable target function method with a conjugate gradient minimization scheme followed by an optional restrained simulated annealing molecular dynamics scheme.

Steady-state kinetics

Steady-state kinetic measurements were conducted at 25°C in assay buffer (50 mM HEPES pH 7.5, 0.5 mM EDTA, containing 0.1 mg/ml ovalbumin and 1 mM DTT). Concentrations of enzymes were 5 nM for UCH L1 and 5 mM for D30K- and C90S-UCH L1 mutants. Ubiquitin-7-amido-4-methylcoumarin (Ub-AMC; Boston Biochem, MA, USA) served as substrate at different concentrations, and AMC production was monitored continuously by fluorescence (Wallace 1420 multilabel counter, Perkin Elmer, Turk, Finland; $\lambda_{ex} = 355$ nm, $\lambda_{em} = 460$ nm). For competition/inhibition by ubiquitin, enzymes were pre-incubated with ubiquitin for 5 min at 25°C before adding substrates. Initial velocity data were used to determine values for K_m, K_i and k_{cat} from non-linear fits of the Michaelis–Menten equation with the program PRISM (GraphPad, San Diego, CA, USA).

ACKNOWLEDGEMENTS

We thank the following people for their contributions to this work: T. Kikuchi, T. Kokubo, R. Takahashi and Y. Imai for helpful discussions; S.-M. Tilghman for kind gift of *Uch l3*$^{A3\text{-}7}$ mouse; T. Kikuchi for technical assistance with tissue sections; A. Kanou for modeling (Ryoka Systems Inc.); K. Arimoto and J. Ando for TOF MASS analysis (Applied Biosystems); F. Melandri (Boston Biochem) for advice regarding steady-state kinetic measurements; S. Kohsaka for providing SH-SY5Y cells; and M. Shikama for the care and breeding of animals. This work was supported by grants-in-aid from the Ministry of Health, Labor and Welfare of Japan, grants-in-aid for scientific research from the Ministry of Education, Culture, Sports, Science and Technology of Japan, a grant from the Organization for Pharmaceutical Safety and Research, and a grant from Japan Science and Technology Cooperation. S.A. is a fellow of the Japan Society for the Promotion of Science (JSPS). Y.-L.W. is a fellow of the Japan Foundation for Aging and Health.

REFERENCES

1. Weissman, A.M. (2001) Themes and variations on ubiquitylation. *Nat. Rev. Mol. Cell. Biol.*, **2**, 169–178.
2. Tran, P.B. and Miller, R.J. (1999) Aggregates in neurodegenerative disease: crowds and power? *Trends Neurosci.*, **22**, 194–197.
3. Wilkinson, K.D., Laleli-Sahin, E., Urbauer, J., Larsen, C.N., Shih, G.H., Haas, A.L., Walsh, S.T. and Wand, A.J. (1999) The binding site for UCH-L3 on ubiquitin: mutagenesis and NMR studies on the complex between ubiquitin and UCH-L3. *J. Mol. Biol.*, **291**, 1067–1077.
4. Larsen, C.N., Krantz, B.A. and Wilkinson, K.D. (1998) Substrate specificity of deubiquitinating enzymes: ubiquitin C-terminal hydrolases. *Biochemistry*, **37**, 3358–3368.
5. Finley, D., Bartel, B. and Varshavsky, A. (1989) The tails of ubiquitin precursors are ribosomal proteins whose fusion to ubiquitin facilitates ribosome biogenesis. *Nature*, **338**, 394–401.
6. Wilkinson, K.D., Lee, K.M., Deshpande, S., Duerksen-Hughes, P., Boss, J.M. and Pohl, J. (1989) The neuron-specific protein PGP 9.5 is a ubiquitin carboxyl-terminal hydrolase. *Science*, **246**, 670–673.
7. Wilkinson, K.D., Deshpande, S. and Larsen, C.N. (1992) Comparisons of neuronal (PGP 9.5) and non-neuronal ubiquitin C-terminal hydrolases. *Biochem. Soc. Trans.*, **20**, 631–637.
8. Lowe, J., McDermott, H., Landon, M., Mayer, R.J. and Wilkinson, K.D. (1990) Ubiquitin carboxyl-terminal hydrolase (PGP 9.5) is selectively present in ubiquitinated inclusion bodies characteristic of human neurodegenerative diseases. *J. Pathol.*, **161**, 153–160.
9. Leroy, E., Boyer, R., Auburger, G., Leube, B., Ulm, G., Mezey, E., Harta, G., Brownstein, M.J., Jonnalagada, S., Chernova, T. *et al.* (1998) The ubiquitin pathway in Parkinson's disease. *Nature*, **395**, 451–452.
10. Saigoh, K., Wang, Y.L., Suh, J.G., Yamanishi, T., Sakai, Y., Kiyosawa, H., Harada, T., Ichihara, N., Wakana, S., Kikuchi, T. *et al.* (1999) Intragenic deletion in the gene encoding ubiquitin carboxy-terminal hydrolase in *gad* mice. *Nat. Genet.*, **23**, 47–51.
11. Kikuchi, T., Mukoyama, M., Yamazaki, K. and Moriya, H. (1990) Axonal degeneration of ascending sensory neurons in gracile axonal dystrophy mutant mouse. *Acta. Neuropathol. (Berl.)*, **80**, 145–151.
12. Wilkinson, K.D. (1997) Regulation of ubiquitin-dependent processes by deubiquitinating enzymes. *FASEB J.*, **11**, 1245–1256.
13. Liu, Y., Fallon, L., Lashuel, H.A., Liu, Z. and Lansbury, P.T. (2002) The UCH-L1 gene encodes two opposing enzymatic activities that affect alpha-synuclein degradation and Parkinson's disease susceptibility. *Cell*, **111**, 209–218.
14. Johnston, S.C., Larsen, C.N., Cook, W.J., Wilkinson, K.D. and Hill, C.P. (1997) Crystal structure of a deubiquitinating enzyme (human UCH-L3) at 1.8 Å resolution. *EMBO J.*, **16**, 3787–3796.
15. Morimoto, T., Ide, T., Ihara, Y., Tamura, A. and Kirino, T. (1996) Transient ischemia depletes free ubiquitin in the gerbil hippocampal CA1 neurons. *Am. J. Pathol.*, **148**, 249–257.
16. Takada, K., Hibi, N., Tsukada, Y., Shibasaki, T. and Ohkawa, K. (1996) Ability of ubiquitin radioimmunoassay to discriminate between mono-ubiquitin and multi-ubiquitin chains. *Biochim. Biophys. Acta*, **1290**, 282–288.
17. Fujimuro, M., Sawada, H. and Yokosawa, H. (1994) Production and characterization of monoclonal antibodies specific to multi-ubiquitin chains of polyubiquitinated proteins. *FEBS Lett.*, **349**, 173–180.
18. Takada, K., Nasu, H., Hibi, N., Tsukada, Y., Ohkawa, K., Fujimuro, M., Sawada, H. and Yokosawa, H. (1995) Immunoassay for the quantification of intracellular multi-ubiquitin chains. *Eur. J. Biochem.*, **233**, 42– 47.
19. Swaminathan, S., Amerik, A.Y. and Hochstrasser, M. (1999) The Doa4 deubiquitinating enzyme is required for ubiquitin homeostasis in yeast. *Mol. Biol. Cell*, **10**, 2583–2594.
20. Amerik, A.Y., Nowak, J., Swaminathan, S. and Hochstrasser, M. (2000) The Doa4 deubiquitinating enzyme is functionally linked to the vacuolar protein-sorting and endocytic pathways. *Mol. Biol. Cell*, **11**, 3365–3380.
21. Johnston, S.C., Riddle, S.M., Cohen, R.E. and Hill, C.P. (1999) Structural basis for the specificity of ubiquitin C-terminal hydrolases. *EMBO J.*, **18**, 3877–3887.
22. Shih, S.C., Sloper-Mould, K.E. and Hicke, L. (2000) Monoubiquitin carries a novel internalization signal that is appended to activated receptors. *EMBO J.*, **19**, 187–198.
23. Nakatsu, F., Sakuma, M., Matsuo, Y., Arase, H., Yamasaki, S., Nakamura, N., Saito, T. and Ohno, H. (2000) A di-leucine signal in the ubiquitin moiety. Possible involvement in ubiquitination-mediated endocytosis. *J. Biol. Chem.*, **275**, 26213–26219.
24. Bennett, M.C., Bishop, J.F., Leng, Y., Chock, P.B., Chase, T.N. and Mouradian, M.M. (1999) Degradation of alpha-synuclein by proteasome. *J. Biol. Chem.*, **274**, 33855–33858.
25. Rochet, J.C. and Lansbury, P.T. Jr (2000) Amyloid fibrillogenesis: themes and variations. *Curr. Opin. Struct. Biol.*, **10**, 60–68.
26. Shimura, H., Hattori, N., Kubo, S., Mizuno, Y., Asakawa, S., Minoshima, S., Shimizu, N., Iwai, K., Chiba, T., Tanaka, K. *et al.* (2000) Familial Parkinson disease gene product, parkin, is a ubiquitin-protein ligase. *Nat. Genet.*, **25**, 302–305.
27. Imai, Y., Soda, M., Inoue, H., Hattori, N., Mizuno, Y. and Takahashi, R. (2001) An unfolded putative transmembrane polypeptide, which can lead to endoplasmic reticulum stress, is a substrate of Parkin. *Cell*, **105**, 891–902.

Downloaded from https://academic.oup.com/hmg/article/12/16/1945/2355580 by guest on 20 August 2022

28. Bizzi, A., Schaetzle, B., Patton, A., Gambetti, P. and Autilio-Gambetti, L. (1991) Axonal transport of two major components of the ubiquitin system: free ubiquitin and ubiquitin carboxyl-terminal hydrolase PGP 9.5. *Brain Res.*, **548**, 292–299.
29. Momose, Y., Murata, M., Kobayashi, K., Tachikawa, M., Nakabayashi, Y., Kanazawa, I. and Toda, T. (2002) Association studies of multiple candidate genes for Parkinson's disease using single nucleotide polymorphisms. *Ann. Neurol.*, **51**, 133–136.
30. Satoh, J. and Kuroda, Y. (2001) A polymorphic variation of serine to tyrosine at codon 18 in the ubiquitin C-terminal hydrolase-L1 gene is associated with a reduced risk of sporadic Parkinson's disease in a Japanese population. *J. Neurol. Sci.*, **189**, 113–117.
31. Wang, J., Zhao, C.Y., Si, Y.M., Liu, Z.L., Chen, B. and Yu, L. (2002) ACT and UCH-L1 polymorphisms in Parkinson's disease and age of onset. *Mov. Disord.*, **17**, 767–771.
32. Maraganore, D.M., Farrer, M.J., Hardy, J.A., Lincoln, S.J., McDonnell, S.K. and Rocca, W.A. (1999) Case-control study of the ubiquitin carboxy-terminal hydrolase L1 gene in Parkinson's disease. *Neurology*, **53**, 1858–1860.
33. Polymeropoulos, M.H., Lavedan, C., Leroy, E., Ide, S.E., Dehejia, A., Dutra, A., Pike, B., Root, H., Rubenstein, J., Boyer, R. *et al.* (1997) Mutation in the alpha-synuclein gene identified in families with Parkinson's disease. *Science*, **276**, 2045–2047.
34. Kitada, T., Asakawa, S., Hattori, N., Matsumine, H., Yamamura, Y., Minoshima, S., Yokochi, M., Mizuno, Y. and Shimizu, N. (1998) Mutations in the parkin gene cause autosomal recessive juvenile parkinsonism. *Nature*, **392**, 605–608.
35. Bonifati, V., Rizzu, P., Van Baren, M.J., Schaap, O., Breedveld, G.J., Krieger, E., Dekker, M.C., Squitieri, F., Ibanez, P., Joosse, M. *et al.* (2002) Mutations in the DJ-1 gene associated with autosomal recessive early-onset Parkinsonism. *Science.* Published online 21 November 2002; 10.1126/science.1077209.
36. Shimura, H., Schlossmacher, M.G., Hattori, N., Frosch, M.P., Trockenbacher, A., Schneider, R., Mizuno, Y., Kosik, K.S. and Selkoe, D.J. (2001) Ubiquitination of a new form of alpha-synuclein by parkin from human brain: implications for Parkinson's disease. *Science*, **293**, 263–269.
37. Abeliovich, A., Schmitz, Y., Farinas, I., Choi-Lundberg, D., Ho, W.H., Castillo, P.E., Shinsky, N., Verdugo, J.M., Armanini, M., Ryan, A. *et al.* (2000) Mice lacking alpha-synuclein display functional deficits in the nigrostriatal dopamine system. *Neuron*, **25**, 239–252.
38. Kurihara, L.J., Semenova, E., Levorse, J.M. and Tilghman, S.M. (2000) Expression and functional analysis of Uch-L3 during mouse development. *Mol. Cell. Biol.*, **20**, 2498–2504.

Downloaded from https://academic.oup.com/hmg/article/12/16/1945/2355580 by guest on 20 August 2022